Oscillation of Angiogenesis with Vascular Dropout in Diabetic Retinopathy by VESsel GENeration Analysis (VESGEN)

Patricia Parsons-Wingerter,[*,1,2] *Krishnan Radhakrishnan,*[2,3] *Mary B. Vickerman,*[1] *and Peter K. Kaiser*[*,4]

Purpose. Vascular dropout and angiogenesis are hallmarks of the progression of diabetic retinopathy (DR). However, current evaluation of DR relies on grading of secondary vascular effects, such as microaneurysms and hemorrhages, by clinical examination instead of by evaluation of actual vascular changes. The purpose of this study was to map and quantify vascular changes during progression of DR by VESsel GENeration Analysis (VESGEN).

Methods. In this prospective cross-sectional study, 15 eyes with DR were evaluated with fluorescein angiography (FA) and color fundus photography, and were graded using modified Early Treatment Diabetic Retinopathy Study criteria. FA images were separated by semiautomatic image processing into arterial and venous trees. Vessel length density (L_v), number density (N_v), and diameter (D_v) were analyzed in a masked fashion with VESGEN software. Each vascular tree was automatically segmented into branching generations ($G_1 \ldots G_8$ or G_9) by vessel diameter and branching. Vascular remodeling status (VRS) for N_v and L_v was graded 1 to 4 for increasing severity of vascular change.

Results. By N_v and L_v, VRS correlated significantly with the independent clinical diagnosis of mild to proliferative DR (13/15 eyes). N_v and L_v of smaller vessels ($G_{\geq 6}$) increased from VRS1 to VRS2 by 2.4 × and 1.6×, decreased from VRS2 to VRS3 by 0.4 × and 0.6×, and increased from VRS3 to VRS4 by 1.7 × and 1.5 × ($P < 0.01$). Throughout DR progression, the density of larger vessels (G_{1-5}) remained essentially unchanged, and D_{v1-5} increased slightly.

Conclusions. Vessel density oscillated with the progression of DR. Alternating phases of angiogenesis/neovascularization and vascular dropout were dominated first by remodeling of arteries and subsequently by veins. (*Invest Ophthalmol Vis Sci.* 2010;51:498–507) DOI:10.1167/iovs.09-3968

Diabetic retinopathy is the leading cause of visual loss among working-aged adults in the United States.[1,2] The diagnosis and management of diabetic retinopathy are based on grading of features obtained from clinical examination, as was performed in the Early Treatment Diabetic Retinopathy Study (ETDRS).[3–5] Although progression of diabetic retinopathy results from adverse vascular remodeling that includes vascular dropout, ischemia, and finally neovascularization, current diagnosis relies on the grading of secondary vascular effects, such as microaneurysms, leakage, and exudates. It is challenging to directly evaluate changes in retinal blood vessels because of the morphologic complexity of the overlapping, highly branching arterial and venous trees within the human retina.

The goal of this study was to investigate changes in the branching patterns of the arterial and venous trees during the progression of diabetic retinopathy. To study vascular remodeling directly, we used VESsel GENeration Analysis (VESGEN) software[6–11] to map and quantify arterial and venous trees extracted from clinical images obtained by fluorescein angiography (FA). The VESGEN computer program analyzes major vascular branching parameters in a binary (black/white) image of a vascular tree, vascular network, or tree-network composite. Mapping and quantification by VESGEN analysis automatically segments vessels within a tree into branching generations (G_1, G_2, … G_x) according to coordinate change in vessel diameter and branching. A recent review[11] of VESGEN applications mapped and quantified vascular trees and networks in the human retina, transgenic mouse retina, and chorioallantoic membrane (CAM), an avian model of angiogenesis and lymphangiogenesis. Coronary vessel development was analyzed as an immature vasculogenic network, a transitional network-tree composite, and a mature tapering vascular tree.

To develop VESGEN mapping capabilities, proangiogenesis and antiangiogenesis factors were first studied in the CAM. By VESGEN analysis, basic fibroblast growth factor (bFGF) stimulated specifically the robust growth of many small vessels.[6] Vascular endothelial growth factor (VEGF)-A, however, had a more complex effect.[9] At low concentrations, VEGF stimulated the growth of new small vessels in a manner resembling stimulation by bFGF. At high concentrations, regulation by VEGF resulted in a more pathologic regulatory phenotype, in which the diameter of larger vessels was significantly dilated (accompanied by vascular leakage). Inhibition of angiogenesis by transforming growth factor (TGF) β-1 retained a normal vascu-

From the [1]National Aeronautics and Space Administration, John H. Glenn Research Center, Cleveland, Ohio; [3]Department of Pathology and Cancer Center, University of New Mexico School of Medicine, Albuquerque, New Mexico; and [4]Cole Eye Institute, Cleveland Clinic Foundation, Cleveland, Ohio.

[2]These authors contributed equally to the work presented here and should therefore be regarded as equivalent authors.

Supported by National Eye Institute Grants R01EY17529 (PP-W) and R01EY17528 (PKK) and NASA Glenn Internal Research and Development Award IRD04–54 (PP-W).

Submitted for publication May 11, 2009; revised July 31, 2009; accepted August 19, 2009.

Disclosure: **P. Parsons-Wingerter**, None; **K. Radhakrishnan**, None; **M.B. Vickerman**, None; **P.K. Kaiser**, None

*Each of the following is a corresponding author: (VESGEN analysis) Patricia Parsons-Wingerter, National Aeronautics and Space Administration, John H. Glenn Research Center, MS 110–3, Cleveland, OH 44135; patricia.a.parsons-wingerter@nasa.gov.
(Clinical) Peter K. Kaiser, Cole Eye Institute, Cleveland Clinic Foundation, Desk i32, 9500 Euclid Avenue, Cleveland OH 44195; pkkaiser@aol.com.

lar morphology,[7] whereas inhibition by angiostatin rendered the vascular tree highly abnormal and irregular.[12] The steroid drug triamcinolone acetonide (TA) also inhibited the growth of small vessels and, furthermore, thinned the diameters of all vessels throughout the vascular tree except those of the smallest vessels.[10]

We have previously quantified, with the use of fractal analysis, vascular morphology in the retinas of patients with normal eyes and those with mild nonproliferative diabetic retinopathy (NPDR).[13] That study showed that compared with the normal retina, the combined density of arteries and veins in the NPDR retina decreased in the macula but was unchanged in peripheral regions. In our present study of progressive vascular remodeling during diabetic retinopathy, VESGEN software mapped and quantified branching characteristics of separated arterial and venous trees to reveal generation-specific changes of oscillating vessel density.

Materials and Methods

Clinical Study

After Cleveland Clinic Foundation Institutional Review Board approval, consecutive patients were prospectively enrolled in this cross-sectional study if they met the following inclusion criteria: age older than 18 years, clinical evidence of mild or greater NPDR based on dilated fundus examination by an experienced retina specialist (PKK), ability to give written informed consent, and no contraindication to fluorescein imaging. Our research in human subjects adhered to the tenets of the Declaration of Helsinki. All patients were imaged by experienced retinal photographers with color fundus photographs and 50° fluorescein angiography (FA). Color fundus photographs were graded and ranked, in a masked fashion by PKK, in order of increasing severity of retinopathy with the use of a modified ETDRS protocol.[3–5]

Angiography was performed by injection of fluorescein into the vasculature, followed by fluorescence imaging of progressive filling of the retinal vasculature. FA images were saved as digital grayscale images (2392 × 2048 pixels). The peak transit images of the FA were graded in a masked fashion by PKK. Given the highly detailed image analysis capabilities of the VESGEN software, only fluorescein angiograms judged to be of excellent image quality were selected based on resolution of the critically important smaller vessels. Only one FA was excluded from analysis based on image-processing grounds because of insufficient resolution of small vessels at higher zoom ratios. FA images were also graded in a masked fashion by PKK and were placed in order based on the severity of ischemia and the status of capillary perfusion in the foveal avascular zone (FAZ).

Initially, 13 eyes from 12 patients were independently graded using the ETDRS criteria as two with mild NPDR, five with moderate NPDR, five with severe NPDR, and one with early PDR. To obtain a minimum statistical sampling of $n = 3$ for each analysis group as classified by vascular remodeling status, two additional FAs (one mild NPDR and one PDR) were included for a total of 15 study eyes. The ranking of eyes in order of increasing severity of diabetic retinopathy was performed in a masked, independent fashion by PKK after VESGEN analysis of all 15 images.

Image Processing

Images acquired at the stage of full arteriovenous filling were selected for VESGEN analysis because our goal was to analyze both arterial and venous trees. The original FA grayscale images (2392 × 2048 pixels) were processed into binary images using 30-inch monitors (Cinema HD Display; Apple, Cupertino, CA; highest resolution, 2560 × 1600 pixels) at several zoom ratios, affording almost one-to-one pixel correspondence. Within each FA image, a vascular pattern of overlapping arterial and venous trees was first extracted by semiautomatic computer processing, as described previously, now using image editing software (Photoshop; Adobe, Mountain View, CA) because of the layering and opacity capabilities.[6–13] The grayscale FA image was first inverted so that the blood vessels appeared dark. Image contrast was optimized to obtain maximal contrast of small vessels by the brightness/contrast tool. A duplicate of the contrast-enhanced image was transformed to a binary image with the thresholding tool to maximally retain larger vessels and some small vessels. Final selection of vessel morphology was accomplished by placing this image above the contrast-enhanced layer and, to maximize visibility of both layers, converting vessels from black to red at a reduced opacity and deleting the white background. The pencil and eraser tools were used to define vessel edges and erase some areas of red background. The red image was converted to black vessels and white background with the magic wand and fill tools, thereby yielding the final binary (black/white) vascular pattern.

The vascular pattern was separated into arterial and venous trees according to comparison with earlier and later images in the FA series to identify various stages of arteriovenous filling of injected fluorescein dye by which arteries are filled before veins; characteristic arterial and venous morphology; reference to the color fundus images in which arteries are more red and veins more purple; and basic principles of vascular tree connectivity, branching, and tapering. For example, arterial and venous trees tend to originate from the optic disc in pairs. Arterial vessels are of smaller diameter than venous vessels and are often more tortuous. VESGEN currently analyzes only two-dimensional images of vascular pattern. Therefore, vessels originating at the optic disc were cut off where they appeared to bend out of the *x-y* image plane into the *z*-plane of the optic nerve. Small vessels supplying only the immediate region of the optic nerve were also excluded. Once a vascular tree was identified as arterial or venous, the tree was followed from its origin to its termination at the smallest generations according to vessel connectivity, bifurcational branching, and tapering (morphologic characteristics of a mature vascular tree). Vessels that appeared to be nonpatent (i.e., without blood flow) because of occlusion, remodeling, or location within hemorrhagic regions were excluded from the binary vascular pattern. Vessel interpretation was decided by agreement between two experienced image processors, subject to final decision by the senior processor.

Vascular Quantification

VESGEN (mature beta version 1.0) is an automated, user-interactive JAVA-based computer code that will be publicly available in the near future, after the development of user documentation. The software operates as a plug-in to ImageJ software (developed by Wayne Rasband, National Institutes of Health, Bethesda, MD; available at http://rsb.info.nih.gov/ij/index.html). The single input image required by VESGEN for mapping and quantification of vascular trees, networks, or tree-network composites is a binary (black/white) image of vascular pattern (Fig. 1). For measurement of density-based parameters, VESGEN optionally imports a user-supplied image defining the region of interest (ROI; illustrated by the black circular regions; see Figs. 3, 4).

Output parameters generated by VESGEN include vessel number density (N_v), vessel length density (L_v), vessel area density (A_v), vessel branch point density (Br_v), vessel tortuosity (T_v), fractal dimension (D_f), and vessel diameter (D_v) for branching generations G_1, G_2, … G_x. For example, D_{v1-5} denotes D_v with respect to branching generations G_1–G_5. Skeletonized (linearized) mappings are used to quantify N_v, L_v, and Br_v. The skeleton is a linearized map of vessel connectivity in which diameters of vessels are reduced to the width of a single pixel. By comparing morphologic characteristics of the input vascular pattern image and its skeleton image as the first mapping output, VESGEN maps the vessel generations (G_1–G_9 for this study; see Figs. 3, 4) and then quantifies vessel density parameters such as L_v and N_v by referring to the ROI input image. A trimmed skeleton excludes linear elements of vessel skeletons lying within the diameters of adjacent vessels, thereby providing precise measurements of L_v and D_v for specific branching generations such as L_{v1}.[8,11] Density functions such as N_v, L_v,

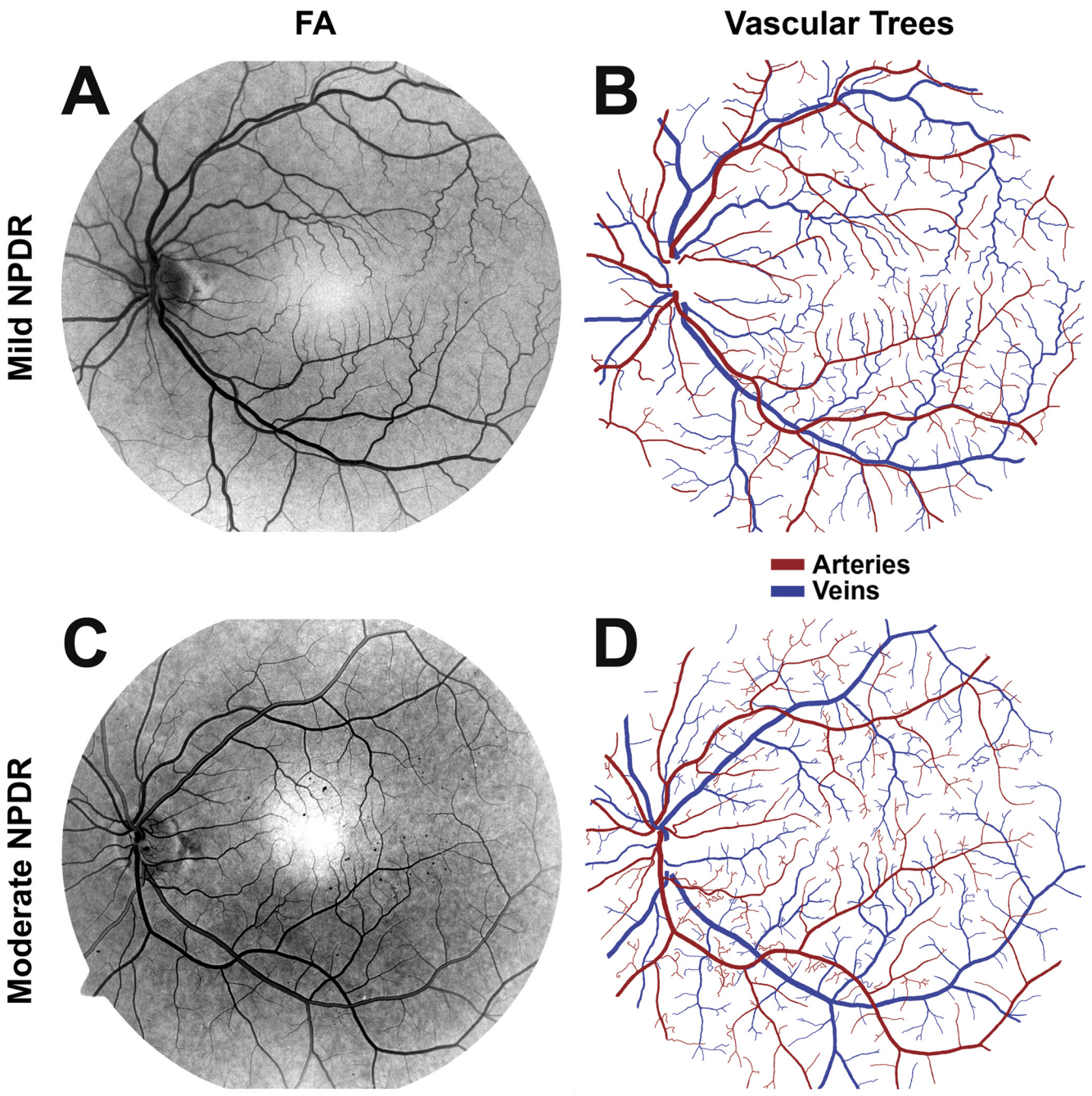

FIGURE 1. Mild and moderate stages of NPDR. Arterial and venous trees extracted from FA images of retinas diagnosed as having mild NPDR (**A**) and moderate NPDR (**C**) are displayed as overlapping vascular patterns (**B**, **D**). Although the trees are shown in *red* and *blue* for illustration, the image of a single isolated tree is imported into VESGEN as a binary (*black/white*) image. To preserve visualization of the critically important small blood vessels, the images are presented in two figures (see Fig. 2 for later stages of diabetic retinopathy). The FAs of Figures 1 and 2 were selected as illustrations because their VESGEN results and clinical ranking are median values for their groups (and close to mean values of vascular density by N_v and L_v; Figs. 5, 6).

A_v, and Br_v are obtained by normalization to the surface area of the ROI (Figs. 3, 4).

Vessel branching generations (G_1–G_x) are determined by VESGEN according to relative decreases in vessel diameter, as first established for branching vascular networks of the dog and pig heart and lung.[14–16] Blood flow velocity is conserved at a symmetric vessel bifurcation, where the diameter of a symmetric offspring vessel decreases to 71% ($1/\sqrt{2}$) of the diameter of the parent vessel. A decrease of vessel diameter to 71% was, therefore, used as the primary determinant of a new branching generation. However, as seen in biological branching trees (Figs. 1–4), the branching of relatively symmetric offspring vessels is not perfectly symmetric, the diameters of very few offspring vessels are of the 71% ideal value, and vessels almost invariably taper. To accommodate a reasonable range of vessel diameters within a biological (nonmathematical) branching generation, VESGEN contains a 15% default tolerance factor that is user-adjustable; the default value was used for this study. The most frequent branching event in a vascular tree is generally the asymmetric offshoot branching

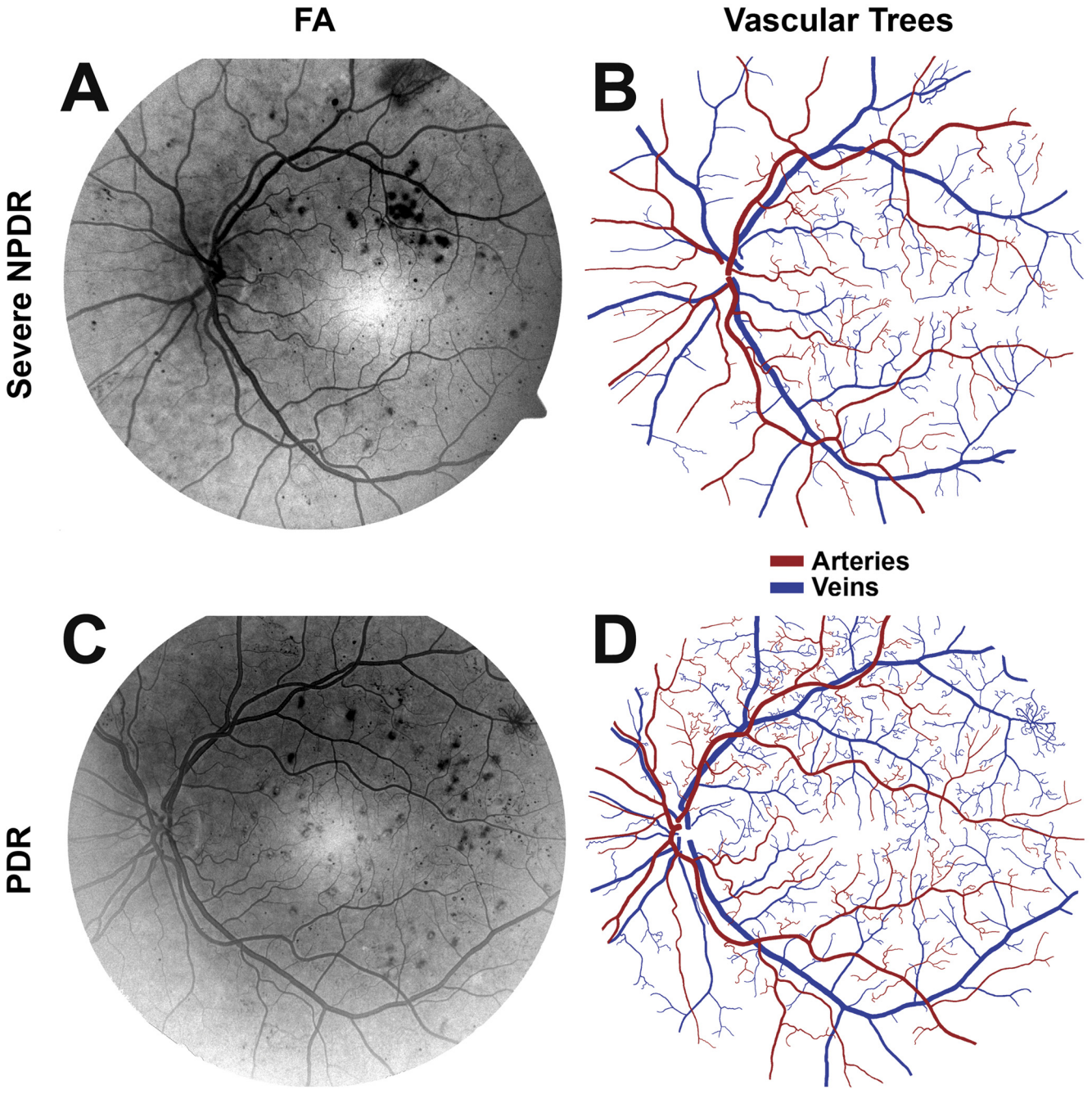

FIGURE 2. Severe NPDR and early PDR. Arterial and venous trees extracted from FA images of retinas diagnosed as having severe NPDR (**A**) and PDR (**C**) are displayed as overlapping vascular patterns (**B**, **D**). As for Figure 1, the FAs were selected because VESGEN results and clinical rankings are median values (Figs. 5, 6).

of a much smaller vessel from a larger vessel, presumably because of space-filling requirements of the tissue for vascular branching.

A preliminary grouping study of arterial vessel density using two images of sparse vessels (severe NPDR) and two images of dense vessels (moderate NPDR) was performed. Results showed that the grouping of large (G_1–G_3) and medium (G_4–G_5) vessels together as (G_1–G_5) and a second grouping of all small vessel generations as $G_{\geq 6}$ were optimal for quantifying where remodeling events fundamentally differed within the branching tree. As described in Results, vascular remodeling status (VRS) was obtained from the VESGEN results for vessel density by N_v and L_v compared with the progressive clinical ranking of the 15 eyes by increasing severity of diabetic retinopathy. Four stages of vascular remodeling status were identified from the N_v and L_v results for the mild NPDR to the very severe NPDR/PDR images and were labeled VRS1 to VRS4 to correspond with increasing severity of diabetic retinopathy. Presentation of our results, therefore, distinguishes among mild NPDR, moderate NPDR, severe NPDR, and very severe NPDR/PDR, as determined by ETDRS clinical diagnosis, and vascular remodeling status VRS1 to VRS4, as determined by VESGEN analysis.

Statistical Analysis

Variation was assessed by calculating the mean ± SE (equal to SD divided by the square root of sample number) and by *P* values from a

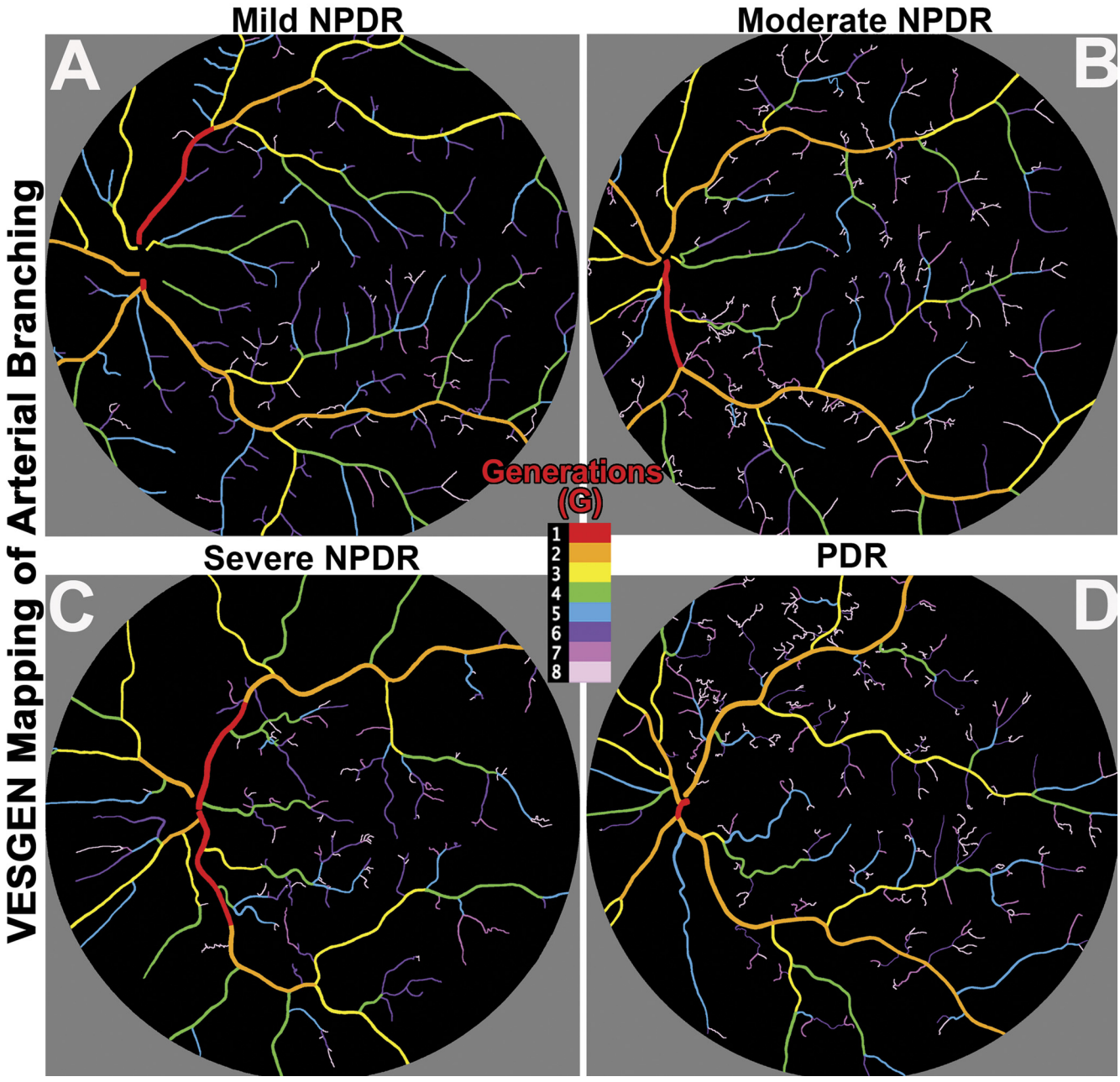

FIGURE 3. Oscillation of arterial density. Eight branching generations (G_1–G_8) were mapped within arterial patterns by VESGEN (Figs. 1, 2). Vessel density increased from mild NPDR (**A**) to moderate NPDR (**B**), decreased at severe NPDR (**C**), and increased again at PDR (**D**) stages of DR. The arterial maps, therefore, display an oscillation between the opposing vascular phenotypes of angiogenesis (or neovascularization) and vascular dropout. Imaging fields for the FAs vary slightly with each photograph, but normalizing vessel density parameters by the ROI corrects for this small variation. In these illustrations, diameters of smaller vessels ($G_{\geq 4}$) were enlarged by two pixels to increase visibility.

Student's *t*-test of equal variance ($\alpha = 0.05$) using Microsoft software (Excel; Redmond, CA). A one-tailed test estimated whether expected decreases or increases between groups were significant; a two-tailed test estimated confidence in overall differences (whether increased or decreased).

RESULTS

Vessel density oscillated with progression from mild NPDR to very severe NPDR/early PDR by alternately displaying angiogenesis and vascular dropout phenotypes, as mapped and quantified by VESGEN. By visual inspection, the vessel density of both arterial and venous trees appeared to increase significantly from mild to moderate NPDR, decrease from moderate to severe NPDR, and increase again from severe to very severe NPDR/early PDR (Figs. 1–4). This alternation or oscillation was observed in the vascular patterns extracted from the FA images (Figs. 1, 2) but was clearly more apparent in the VESGEN maps of generational branching (Figs. 3, 4).

Progression of vascular remodeling as measured by N_v and L_v for all vessels within an arterial or a venous tree image correlated significantly, but not absolutely, with ranked progression by clinical diagnosis (13/15 eyes; Fig. 5). N_v and L_v generally confirm each other as indicators of the space-filling

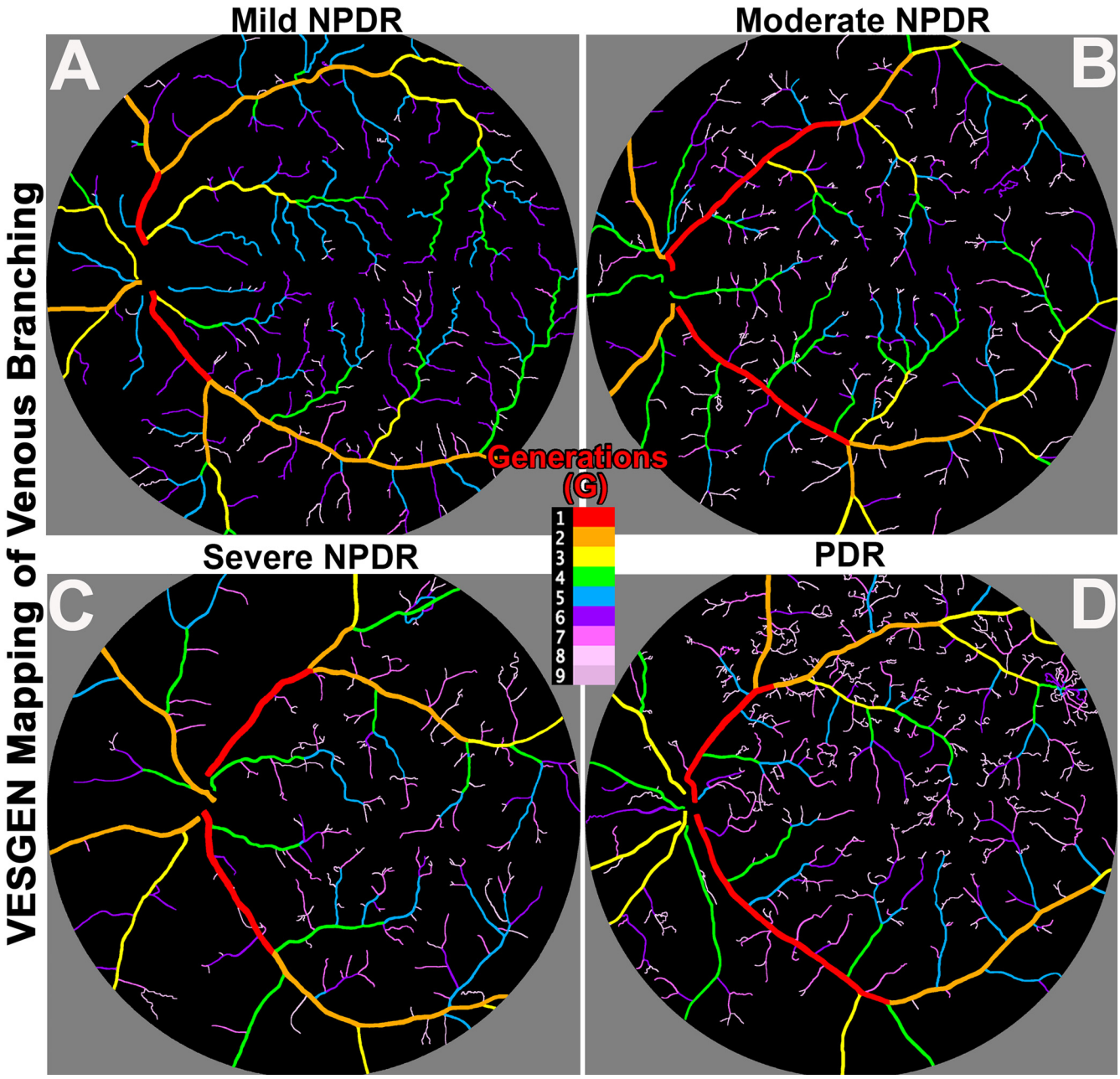

FIGURE 4. Oscillation of venous density. Eight or nine branching generations (G_1–G_8 or G_9) were mapped within venous patterns by VESGEN (Figs. 1, 2). Vessel density increased from mild NPDR (**A**) to moderate NPDR (**B**), decreased at severe NPDR (**C**), and again increased at PDR (**D**) stages of DR. Venous maps appear to correlate positively with results for arterial maps (Fig. 3). The diameters of small veins ($G_{\geq 4}$) were enlarged by two pixels for improved visibility.

capacity of a branching tree.[10] Grouping by arterial results for N_v (Fig. 5A) was particularly clear and provided the primary basis for defining the VRS as VRS1 to VRS4, corresponding to increasing severity of diabetic retinopathy (confirmed by all other results; Fig. 5). In particular, the VRS groups of 1, 2, 3, and 4, as defined by N_v and L_v, correlate positively with ETDRS diagnoses of mild NPDR, moderate NPDR, severe NPDR, and very severe NPDR/PDR. Significantly, two arterial trees that ranked highest in the clinically diagnosed groups of moderate NPDR and severe NPDR were clearly reclassified by arterial remodeling status (Fig. 5A) as VRS3 (eye 8) and VRS4 (eye 13). Vascular changes for reclassification into a more advanced stage are more apparent at an earlier clinical stage of diabetic retinopathy in arterial trees than in venous trees, for both N_v and L_v (Fig. 5). Nonetheless, the ranked clinical diagnosis based on secondary vascular features provided a necessary first-round sorting or binning of disease progression, before subsequent grouping by vascular remodeling status, as determined by N_v and L_v. Grading of the vascular remodeling status by N_v or L_v may be helpful for improved, predictive diagnosis and treatment but would not be sufficient to grade DR progression because of the non-uniqueness of groups (i.e., vessel density of VRS1 resembles that of VRS3, and vessel density of VRS2 resembles that of VRS4).

Capillary nonperfusion in the FA was evaluated for correlation with disease progression. The perfusion status of the FAZ,

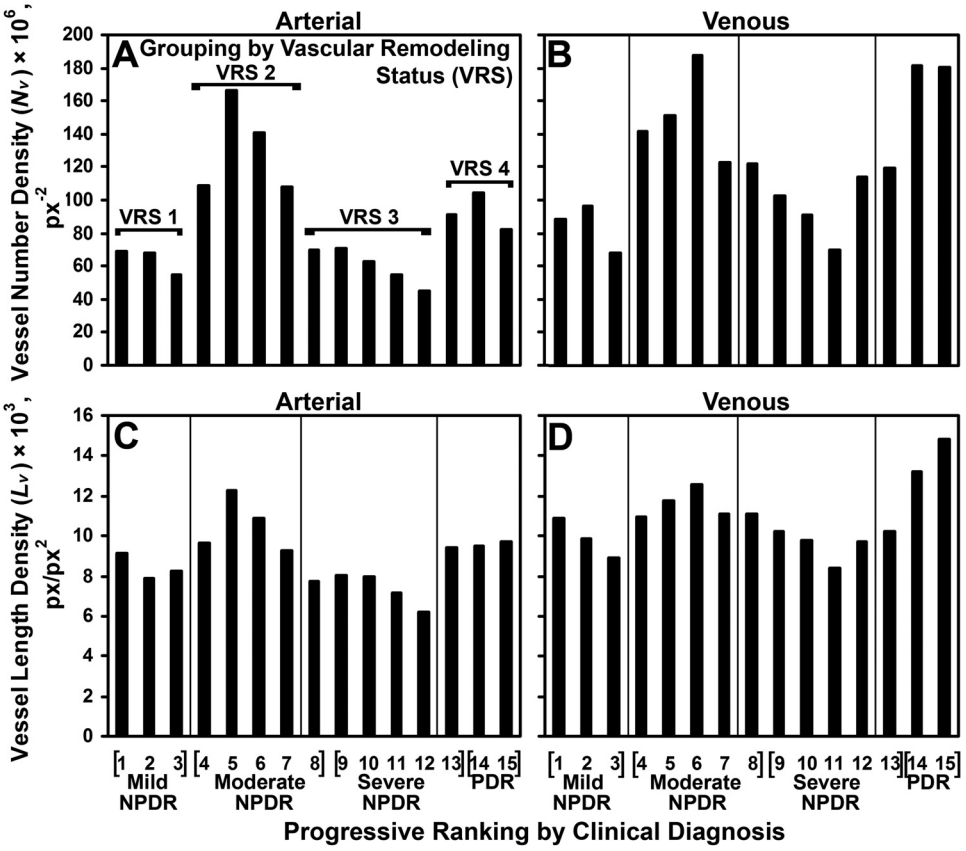

FIGURE 5. Grouping of VRS by ranking of clinical diagnosis and VESGEN results. To determine appropriate analysis groups of progressive vascular remodeling for subsequent VESGEN quantification, the FAs were ranked by clinical diagnosis from 1 to 15, in order of increasing severity of diabetic retinopathy. Diagnosis was based on modified ETDRS clinical criteria that included density and location of microaneurysms, hemorrhagic leakage, exudates, ischemic areas, neovascularization, and vascular arcades. The density of all vessels (overall density) determined by VESGEN was plotted and compared with clinical ranking. Vessel number density (N_v) and vessel length density (L_v) are excellent measures of the space-filling capacity of tree-branching patterns. Results clearly reveal oscillation between angiogenesis and vascular dropout as a direct, positive function of clinically diagnosed progression of diabetic retinopathy. The plots show good agreement for these oscillatory trends between arterial and venous trees and between N_v and L_v. According to arterial results for N_v (**A**), the highest-ranking patients for the clinically diagnosed moderate and severe groups (eyes 8 and 13) were reclassified by vascular remodeling status as VRS3 (correlated to severe NPDR) and VRS4 (correlated to very severe NPDR/PDR). Because of the clear binning of clinically ranked grading and dominance of arterial remodeling compared with venous remodeling during the first angiogenic phase (mild to moderate), arterial results for N_v were used to define the four analysis groups, VRS1 to VRS4. *Black vertical lines* indicate this grouping of arterial and venous trees by vascular remodeling status into VRS1 to VRS4.

shown in Table 1, is compared with the ETDRS diagnosis and VRS obtained from VESGEN results and is ordered by increasing severity of diabetic retinopathy, as for Figure 5. The positive correlation of FAZ perfusion status with VRS and ETDRS diagnosis is strong but not absolute. Significant differences between perfusion status and vascular changes analyzed by ETDRS and VESGEN include two eyes diagnosed as mild NPDR (eyes 1 and 3) that display a normal perfusion status, whereas a third eye, also diagnosed as mild NPDR (eye 2), showed moderate enlargement. Normal perfusion status was also noted in an eye diagnosed with severe NPDR (eye 12). Thus, FAZ perfusion status did not necessarily correlate with ETDRS retinopathy scores.

TABLE 1. ETDRS Diagnosis and VRS Compared with Perfusion Status of FAZ

Eye No.	ETDRS Diagnosis	VRS	Perfusion Status of FAZ
1	Mild	1	Normal
2	Mild	1	Mild enlargement
3	Mild	1	Normal
4	Moderate	2	Mild enlargement
5	Moderate	2	Mild enlargement
6	Moderate	2	Normal
7	Moderate	2	Mild enlargement
8	Moderate	3	Moderate enlargement
9	Severe	3	Mild enlargement
10	Severe	3	Moderate enlargement
11	Severe	3	Moderate enlargement
12	Severe	3	Normal
13	Severe	4	Moderate enlargement
14	PDR	4	Severe enlargement
15	PDR	4	Severe enlargement

The ETDRS clinical grading and capillary perfusion status of the FAZ were provided in a masked fashion. The VRS was obtained from the VESGEN results for arterial number and length densities (Fig. 5). The eyes are ordered by increasing severity of diabetic retinopathy according to ETDRS diagnosis. The positive correlation of perfusion status with VRS and ETDRS diagnosis is strong but not absolute.

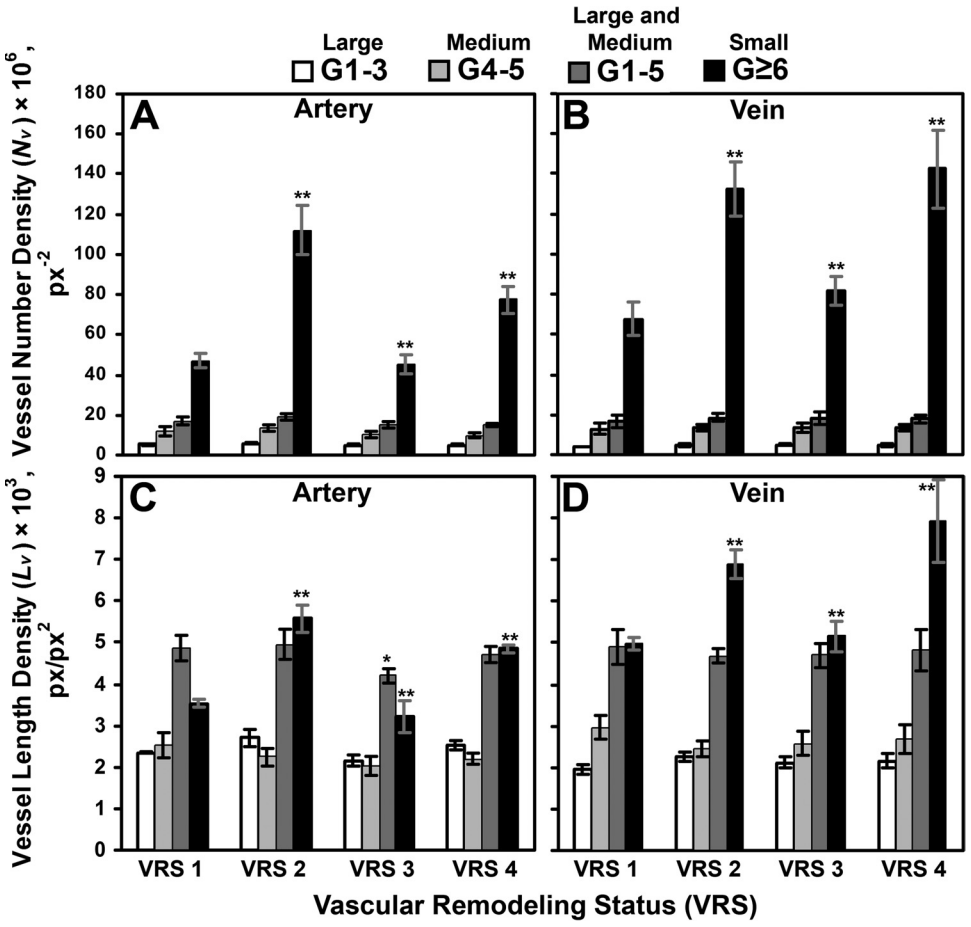

FIGURE 6. By VESGEN analysis, angiogenesis and vascular dropout oscillate with progressive vascular remodeling of smaller arteries and veins. By N_v and L_v, the oscillation between angiogenesis and vascular dropout during diabetic retinopathy were restricted to smaller blood vessels ($G_{\geq 6}$), as quantified by changes in vessel density during progression of vascular remodeling status from VRS1 to VRS4. Relative increases in vessel density by N_v and L_v were greater for arteries than for veins in the first phase of angiogenesis (VRS1-VRS2) but greater for veins in the second phase of angiogenesis (VRS3-VRS4). Data are plotted as mean ± SE. $^*P \leq 0.05$ and $^{**}P \leq 0.01$, one-tailed *t*-test, for confidence estimation of either increased or decreased vessel density for G_{1-5} and $G_{\geq 6}$ from VRS1 to VRS2, VRS2 to VRS3, and VRS3 to VRS4. By a two-tailed *t*-test (for estimation of confidence in differences), *P*-values of $N_{v\geq 6}$ and $L_{v\geq 6}$ for all arterial and venous transitions were ≤0.01, except arterial and venous $L_{v\geq 6}$ for VRS3 to VRS4, which were 0.02.

When grouped by vascular remodeling status (Fig. 6), the density of smaller vessels ($G_{\geq 6}$) by N_v and L_v increased up to 2.4× from VRS1 to VRS2, decreased by as much as 0.4× from VRS2 to VRS3, and increased up to 1.74× from VRS3 to VRS4 (all for N_v, $P < 0.01$). The density of larger vessels (G_{1-5}) did not change significantly during vascular remodeling (all $P \gg 0.05$ by two-tailed *t*-test; Fig. 6). Hence, by correlation of vascular remodeling status with ranked clinical diagnosis, diabetic retinopathy appeared to progress by net angiogenesis from mild to moderate NPDR, by net vascular dropout from moderate to severe NPDR, and by net angiogenesis/neovascularization from severe to very severe NPDR/early PDR (Figs. 1–4).

Increases in the diameters of larger arteries and veins (D_{v1-5}) appeared to be small but consistent throughout the progression of diabetic retinopathy (Fig. 7). For smaller vessels, $D_{v\geq 6}$ was relatively constant, at least at this level of image resolution, whereas smaller vessels measured only several pixels in diameter. Vessel area density (A_v) measured the coupled effects of space-filling branching (L_v) and vessel width (D_v) because it was directly proportional to $L_v \cdot D_v$. Therefore, results for A_v (not shown) in this study were not particularly helpful given the contrasting trends for L_v and D_v.

In the first phase of angiogenesis (i.e., progression from VRS1 to VRS2), the relative increase in density of small arteries

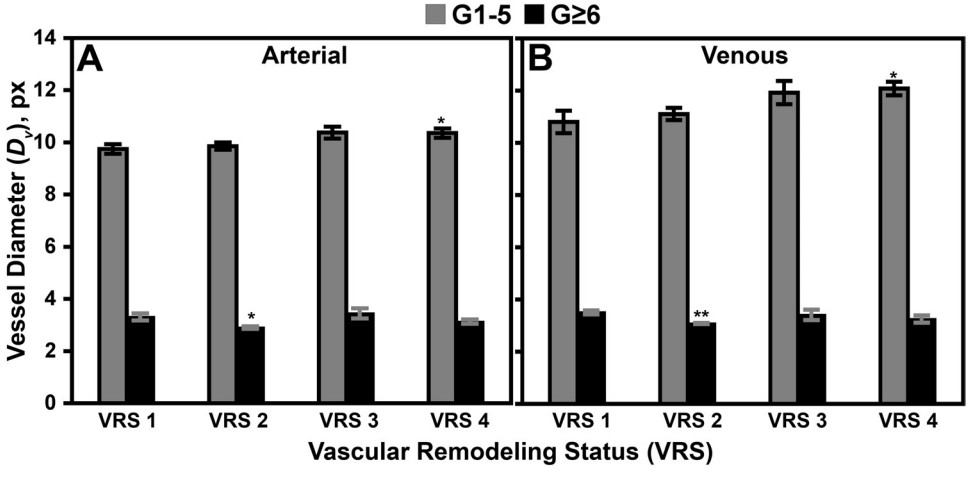

FIGURE 7. By VESGEN analysis, the diameters of large and medium-sized vessels increase with progressive vascular remodeling. By measurements of D_v, the diameters of large and medium-sized arteries and veins (G_{1-5}) increased slightly, but consistently, with progressive vascular remodeling. The diameters of smaller vessels did not appear to vary greatly with disease progression. Data are plotted as mean ± SE. $^*P \leq 0.05$ and $^{**}P \leq 0.01$, one-tailed *t*-test, for confidence estimation of increased diameter during vascular remodeling of VRS2, VRS3, and VRS4 compared with VRS1.

($G_{\geq 6}$) by L_v and N_v was larger than the relative increase of small veins (Fig. 6). However, results were opposite for the second, late-stage phase of angiogenesis/neovascularization (progression from VRS3 to VRS4), when the relative increase in density of small veins exceeded that of small arteries. Furthermore, the final overall increase in D_v of large- and medium-sized veins (G_{1-5}) from VRS1 to VRS4 was greater than that of large- and medium-sized arteries (12% compared to 6%; Fig. 7). Together, these two results for vessel density and vessel diameter suggest a fundamental switch in the second, more severe phase of late-stage angiogenesis from a vascular phenotype of arterial-dominated remodeling to a phenotype of venous-dominated remodeling.

Discussion

The major result of this study was the oscillation (alternation) of increasing and decreasing density of small blood vessels, as mapped and quantified by L_v and N_v, in both arterial and venous trees during progression of diabetic retinopathy from mild to very severe NPDR/early PDR. When classified by VRS, the density of smaller vessels increased from VRS1 to VRS2, decreased from VRS2 to VRS3, and increased again from VRS3 to VRS4, as quantified by VESGEN with strong statistical confidence. The two phases of increased vessel density (VRS1 to VRS2 and VRS3 to VRS4) were dominated first by arterial remodeling and were followed by venous remodeling, although progressive change was always positively correlated between arterial and venous trees. Classification of VRS by vessel density correlated significantly with ranking by clinical diagnosis from mild NPDR to very severe NPDR/early PDR (13/15 eyes). Indeed, vessel densities for the two uncorrelated retinas (eyes 8 and 13) correlated positively with the next phase of retinopathy progression, suggesting that vascular remodeling may be an earlier prognosticator of retinopathy status than secondary vascular effects, such as microaneurysms and hemorrhages. Although the positive correlation of FAZ perfusion status with VRS and ETDRS diagnosis was strong, it was not absolute.

Throughout the progression of diabetic retinopathy, the density of larger vessels (G_{1-5}) remained relatively unchanged, and the diameters of larger vessels (D_{v1-5}) increased slightly but consistently. Results of our small cross-sectional study suggest that a larger longitudinal study would investigate and confirm more conclusively whether arterial remodeling and other vascular morphologic changes precede the appearance of secondary vascular events, such as frequency of microaneurysms and hemorrhagic leakage, currently used for the diagnosis of disease. We chose to work with FAs because of the superior resolution of the critically important smaller blood vessels in comparison with fundus images. In the future, this analysis may also prove useful for good quality fundus images.

Inspection of the VESGEN mappings and binary vascular trees (Figs. 1–4) reveals that changes throughout the retinal vasculature displayed in an FA image are not necessarily uniform with progression of diabetic retinopathy. Therefore, we describe increased vessel density as net angiogenesis, neovascularization, or both and decreased vessel density as net vascular dropout. Vascular change from very severe NPDR to PDR is characterized by neovascularization with increased numbers of vessel structures (primarily venous intraretinal microvascular abnormalities) that are organized as vascular loops rather than by tapered branching. The oscillation between angiogenesis/neovascularization and vascular dropout with the progression of diabetic retinopathy suggests that the diabetic retina retains the capacity to recover a normal vascular phenotype to some extent during earlier stages of retinopathy. Presumably, the cyclical nature of the angiogenesis/vascular dropout process is regulated by competing provascular and antivascular factors such as tissue hypoxia, VEGF, and other stimulatory and inhibitory factors. Identifying what constitutes the various angiogenic "switches"[17] and changing temporal balance among proangiogenic and antiangiogenic vascular stability factors would require highly detailed, complex molecular and cellular biology studies.

In a previous study based on fractal analysis,[13] we found that vessel density decreased in the mild NPDR macular region compared with the normal macula. If the results reported for our current VESGEN study of arterial and venous trees are consistent with results for the previous fractal study of overall vessel density, then the increased vessel density of the moderate NPDR retina would resemble more closely the vascular architecture of the normal, healthy retina than the mild NPDR retina. Vascular dropout in mild NPDR could be the initial phase of significant ischemic injury. We propose that more extensive studies would be of significant value in resolving this important issue. Answers to this question—whether retinal vessels drop out during mild NPDR and recover to some extent during moderate NPDR—could be critical for advances in therapeutic design. Drugs that ameliorate tissue hypoxia, vascular dropout, or early angiogenesis may potentially reverse the progression of diabetic retinopathy during early stages more favorably than in the later stages, when anti-VEGF and other antiangiogenesis therapies are tested.

It is not surprising that oscillation of vessel density with progression of diabetic retinopathy depends primarily on the alternating growth and dropout of smaller, more fragile blood vessels. Research has shown that factors such as VEGF and normoxia are required to stabilize and maintain the smaller blood vessels.[18–20] Moreover, the molecular and cellular characteristics of angiogenic and remodeling vascular tissues differ from those of more mature, stable vascular tissues.[21–23] As shown by VESGEN analysis of numerous growth factors and therapeutics in CAM, stimulation or inhibition of angiogenesis targets the growth of small blood vessels within the vascular tree.[6–10,12]

Despite the generality of inhibition and stimulation at the level of small vessels, each molecular perturbant of angiogenesis elicited a response that was spatiotemporally distinct and quantifiable. Our previous studies of vascular remodeling by VESGEN analysis in the avian CAM experimental model have focused mainly on the mapping and quantifying of unique "fingerprint" or "signature" patterns induced by angiogenic stimulators such as $VEGF_{165}$ and bFGF, and by inhibitors such as TGF-β1, angiostatin, and the steroid TA (provided as background information in the introduction). Results of the CAM studies suggest the hypothesis that progressive changes in the vascular patterns of pathologic angiogenesis and human vascular diseases such as diabetic retinopathy could be analyzed to determine whether molecular signature patterns can be identified that provide integrative readouts of the dominant molecular signaling.

Our hypothesis is consistent with the angiogenesis switch hypothesis proposed by Hanahan and Folkman[17] and others on the multiplicity, variability, and evolving dynamic balance among numerous angiogenic stimulators and inhibitors. In our present study, for example, the switch from the high arterial density and relatively normal diameters of larger arteries at VRS2 (as correlated with moderate NPDR) to lower arterial density and significantly increased diameters of larger arteries at VRS4 (correlated with very severe NPDR/early PDR) corresponds morphologically to changes mapped and quantified by VESGEN for VEGF regulation. Vessel density in the CAM in-

creased at low concentrations of VEGF. With higher concentrations of VEGF, however, the vascular phenotype displayed progressively decreasing vessel density and increasing diameters of larger arteries.[9] Adverse side effects of TA as a therapeutic agent for vascular retinopathies, such as increased risk for glaucoma, could result from the unfavorable thinning of vessel diameters, as demonstrated by experimental results for TA measured by VESGEN in the CAM[10] However, any conclusive deduction of dominant molecular regulation from changing vascular pattern as a dependent readout of progressive DR or other human vascular disease would certainly require much further investigation through numerous, large studies. Finally, the effects of drugs such as TA, pegaptanib (Macugen; Eyetech, New York, NY), ranibizumab (Lucentis; Genentech, South San Francisco, CA), and bevacizumab (Avastin; Genentech, South San Francisco, CA) on retinal vascular pattern could be evaluated by VESGEN to help quantify the degree of vascular normalization achieved by these therapeutics.

Acknowledgments

The authors thank David Jacqmin (NASA Glenn Research Center) for helpful discussion and Dan Gedeon, Alan Hylton, Terri McKay, and Daniela Ribita for helpful technical support.

References

1. Blindness caused by diabetes—Massachusetts 1987–1994. *MMWR Morbid Mortal Wkly Rep*. 1996;45:937–941.
2. National Center for Chronic Disease Prevention and Health Promotion. Diabetes Public Health Resource: National Diabetes Fact Sheet. http://www.cdc.gov/diabetes/pubs/estimates.htm. Accessed September 13, 2009.
3. Grading diabetic retinopathy from stereoscopic color fundus photographs—an extension of the modified Airlie House classification: ETDRS report number 10. Early Treatment Diabetic Retinopathy Study Research Group. *Ophthalmology*. 1991;98:786–806.
4. Classification of diabetic retinopathy from fluorescein angiograms: ETDRS report number 11. Early Treatment Diabetic Retinopathy Study Research Group. *Ophthalmology*. 1991;98:807–822.
5. Fundus photographic risk factors for progression of diabetic retinopathy: ETDRS report number 12. Early Treatment Diabetic Retinopathy Study Research Group. *Ophthalmology*. 1991;98:823–833.
6. Parsons-Wingerter P, Elliott KE, Clark JI, Farr AG. Fibroblast growth factor-2 selectively stimulates angiogenesis of small vessels in arterial tree. *Arterioscler Thromb Vasc Biol.* 2000a;20:1250–1256.
7. Parsons-Wingerter P, Elliott KE, Farr AG, Radhakrishnan K, Clark JI, Sage EH. Generational analysis reveals that TGF-beta1 inhibits the rate of angiogenesis in vivo by selective decrease in the number of new vessels. *Microvasc Res.* 2000b;59:221–232.
8. Parsons-Wingerter P, McKay TL, Leontiev D, Vickerman MB, Condrich TK, Dicorleto PE. Lymphangiogenesis by blind-ended vessel sprouting is concurrent with hemangiogenesis by vascular splitting. *Anat Rec A Discov Mol Cell Evol Biol.* 2006a;288:233–247.
9. Parsons-Wingerter P, Chandrasekharan UM, McKay TL, et al. A VEGF165-induced phenotypic switch from increased vessel density to increased vessel diameter and increased endothelial NOS activity. *Microvasc Res.* 2006b;72:91–100.
10. McKay TL, Gedeon DJ, Vickerman MB, et al. Selective inhibition of angiogenesis in small blood vessels and decrease in vessel diameter throughout the vascular tree by triamcinolone acetonide. *Invest Ophthalmol Vis Sci.* 2008;49:1184–1190.
11. Vickerman MB, Keith PA, McKay TL, et al. VESGEN 2D: automated, user-interactive software for quantification and mapping of angiogenic and lymphangiogenic trees and networks. *Anat Rec (Hoboken).* 2009;292:320–332.
12. Parsons-Wingerter P, Lwai B, Yang MC, et al. A novel assay of angiogenesis in the quail chorioallantoic membrane: stimulation by bFGF and inhibition by angiostatin according to fractal dimension and grid intersection. *Microvasc Res.* 1998;55:201–214.
13. Avakian A, Kalina RE, Sage EH, et al. Fractal analysis of region-based vascular change in the normal and non-proliferative diabetic retina. *Curr Eye Res.* 2002;24:274–280.
14. Gan RZ, Tian Y, Yen RT, Kassab GS. Morphometry of the dog pulmonary venous tree. *J Appl Physiol.* 1993;75:432–440.
15. Kassab GS, Rider CA, Tang NJ, Fung YC. Morphometry of pig coronary arterial trees. *Am J Physiol.* 1993;265:H350–H365.
16. Kassab GS, Lin DH, Fung YC. Morphometry of pig coronary venous system. *Am J Physiol.* 1994;267:H2100–H2113.
17. Hanahan D, Folkman J. Patterns and emerging mechanisms of the angiogenic switch during tumorigenesis. *Cell.* 1996;86:353–364.
18. Huang J, Bae JO, Tsai JP, et al. Angiopoietin-1/Tie-2 activation contributes to vascular survival and tumor growth during VEGF blockade. *Int J Oncol.* 2009;34:79–87.
19. Cai J, Kehoe O, Smith GM, Hykin P, Boulton ME. The angiopoietin/Tie-2 system regulates pericyte survival and recruitment in diabetic retinopathy. *Invest Ophthalmol Vis Sci.* 2008;49:2163–2171.
20. Ramsauer M, D'Amore PA. Contextual role for angiopoietins and TGFβ1 in blood vessel stabilization. *J Cell Sci.* 2007;120:1810–1817.
21. Benjamin LE, Hemo I, Keshet E. A plasticity window for blood vessel remodelling is defined by pericyte coverage of the preformed endothelial network and is regulated by PDGF-B and VEGF. *Development.* 1998;125:1591–1598.
22. Gerhardt H, Golding M, Fruttiger M, et al. VEGF guides angiogenic sprouting utilizing endothelial tip cell filopodia. *J Cell Biol.* 2003;161:1163–1177.
23. Ahmed Z, Bicknell R. Angiogenic signalling pathways. *Methods Mol Biol.* 2009;467:3–24.